# Amplitude dropout in coupled lasers

A. I. Khibnik,[1] Y. Braiman,[2] V. Protopopescu,[2] T. A. B. Kennedy,[3] and K. Wiesenfeld[3]
[1]*United Technologies Research Center, 411 Silver Lane, MS 129-15, East Hartford, Connecticut 06108*
[2]*Center for Engineering Science Advanced Research, Computer Science and Mathematics Division, Oak Ridge National Laboratory, Oak Ridge, Tennessee 37831*
[3]*School of Physics, Georgia Institute of Technology, Atlanta, Georgia 30332*
(Received 8 May 2000; revised manuscript received 9 August 2000; published 15 November 2000)

We study the entrainment of coupled solid-state lasers by an external injected field. We show that the total output intensity exhibits unexpected nonmonotonic behavior as a function of the injected field and find the critical amplitude marking the transition to the low-intensity branch. In addition, we also show that substantial partial entrainment can be achieved for injected fields much weaker than that required for full entrainment.

PACS number(s): 42.55.−f, 05.45.Xt, 42.60.Da, 42.60.Fc

Laser arrays are promising for applications that require high optical power from a compact source [1–3]. Both solid-state [4–7] and semiconductor [8–12] arrays are subjects of intense research, and various aspects of their dynamical behavior such as chaotic synchronization [13] and chaotic communication [14] have already been reported.

The most efficient mode of operation is realized when the elements are synchronized such that the output interferes constructively and the light intensity is maximized. Unfortunately, this synchronized state is typically unstable. Instead, the attracting dynamics is the out-of-phase state, leading to destructive interference resulting in low output intensities [7,8,11].

To date, various techniques have been proposed to obtain stable in-phase behavior. A potentially useful technique is to inject a common driving laser field into the laser array elements [7,11,15,16]. For sufficiently high driving amplitude, the elements are entrained and interfere constructively; full entrainment of the array is realized above a certain value determined by the coupling of the array elements [7,11]. On the other hand, as a practical matter, this technique would become more powerful if entrainment were achieved with relatively low driving amplitudes.

In this paper, we elucidate a newly observed dynamical behavior of a two-laser array under external injection, namely, a strongly nonmonotonic behavior of the output intensity as a function of the injected field. We show that significant entrainment can be achieved even for relatively small injected fields; this feature has obvious practical relevance. To the best of our knowledge, the first numerical evidence of a nonmonotonic response in two coupled lasers has been recently reported by Khibnik *et al.* [17]. A nonmonotonic response of the sliding velocity to the applied force in a two-dimensional (2D) driven array of Frenkel-Kontorova-type oscillators was recently reported in numerical simulations by Braun *et al.* [18]. Both results suggest that nonmonotonocity is intrinsic for a broad range of diverse fields (such as lasers, atomic scale devices, Josephson junctions) that can be modeled in terms of nonlinear coupled oscillators.

Starting from the complete equations of motion for the laser array, we first provide a rigorous reduction of the complete array dynamics to a simpler description. The reduced equations fall into a class of dynamical models known as phase models [17,19,20]. Based on the phase model, we provide a complete analytical understanding of the nonmonotonic behavior of total output intensity of the laser array as a function of the injected field and calculate the strength of the injected field where the abrupt transition to much lower intensity occurs.

Our starting point is the system of equations describing the dynamics of two evanescently coupled solid-state lasers, where the polarization is adiabatically eliminated:

$$\dot{E}_j(t) = (G_j - \alpha_j + \imath\,\delta_j)E_j + \kappa(E_{j+1} + E_{j-1}) + E_e(t),$$

$$\dot{G}_j(t) = \frac{\tau_c}{\tau_f}[p_j - (1 + |E_j|^2)G_j], \tag{1}$$

where $j=1,2$, and free end boundary conditions $[E_0(t) = E_3(t) = 0]$ are imposed. The variables $E_j$ and $G_j$ are the dimensionless complex electric field and gain for the $j$th laser. All times and frequencies are scaled relative to the cavity round trip time, $\tau_c$, and $\tau_f$ is the fluorescence time of the laser medium; $\alpha_j$ and $p_j$ are the dimensionless cavity decay and pump rates for the $j$th laser, respectively, $\kappa$ is the evanescent coupling constant between the two lasers, and $E_e(t)$ is the slowly varying amplitude of the external field which drives each laser [9]. Equations (1) are written in a frame rotating with frequency $\omega_e$, at which the external field has a nonzero Fourier component. This frequency is tuned to minimize the detuning from the cavity resonances. In practice, the output power emitted from an array depends on the tuning of external field to the cavities [16]. The detuning $\delta_j = \omega_e - \omega_{cj} - G_j\Delta\omega_j \approx \omega_e - \omega_{cj}$, where $\omega_{cj}$ is the cavity resonance frequency for laser $j$ and $\Delta\omega$ is the atomic detuning from $\omega_e$ in units of the polarization decay rate. For solid-state lasers, the latter dynamic contribution to the detuning is generally ignored. In the following, we allow for a small spread in detunings as a way to test the robustness of the entrainment mechanism to a physically reasonable parameter spread.

We assume $\alpha_j = \alpha$, $p_j = p$, $p > \alpha$ [7]. Substituting $E_j(t) = \sqrt{I_j(t)}\exp(i\,\phi_j(t))$, where $I_j(t)$ and $\phi_j(t)$ are the intensity

 

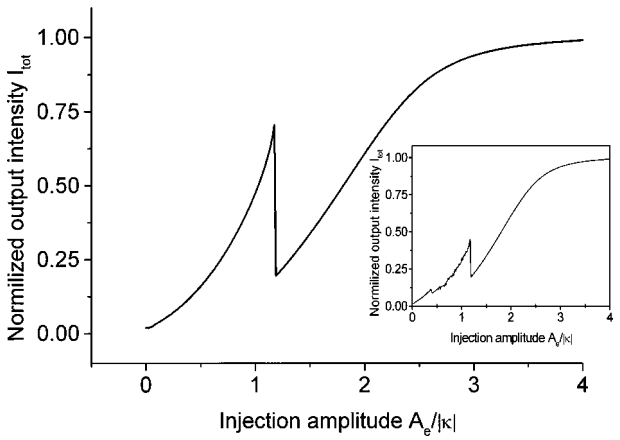


FIG. 1. The normalized total intensity, $I_{\mathrm{tot}}=(1/4I)|(E_1+E_2)|^2$, as a function of the strength of the dimensionless injected field, $A_e=\sqrt{I_e/I}$. The curve was computed by gradually increasing the amplitude of the injected field. An inset shows the *average* normalized total intensity, $I_{\mathrm{tot}}$, as a function of $A_e$. Our statistical average is based on 500 simulations, each performed using a different set of initial conditions. The other parameters are $\alpha=0.01$, $p=0.015$, $\kappa=-10^{-5}$, $\omega_0=5\times10^{-7}$, $\delta_1=28.18\times10^{-7}$, and $\delta_2=-26.8\times10^{-7}$. The entrainment amplitude $A_{\mathrm{entr}}/|\kappa|=4$. All units are dimensionless.

and the phase of laser $j$ and assuming $E_e(t)=E_e\equiv\sqrt{I_e}$ to be a constant field, the model equations for two lasers read

$$\dot{I}_j=2(G_j-\alpha)I_j+2\kappa\sqrt{I_1I_2}\cos(\phi_2-\phi_1)+2\sqrt{I_eI_j}\cos\phi_j,$$

$$\dot{\phi}_j=\delta_j+(-1)^j\kappa\frac{\sqrt{I_1I_2}}{I_j}\sin(\phi_1-\phi_2)-\sqrt{\frac{I_e}{I_j}}\sin\phi_j, \quad (2)$$

$$\dot{G}_j=(p-G_j-G_jI_j)\omega_0,$$

where $\omega_0=\tau_c/\tau_f$. Throughout the paper, we set $\alpha=0.01$, $p=0.015$, $\kappa=-10^{-5}$, $\omega_0=5\times10^{-7}$, and we vary only $\delta_1$, $\delta_2$, and $I_e$.

Equations (2) have been studied theoretically for $N$ coupled lasers [7] and the condition for full entrainment has been derived. This condition assumes small deviations in detunings and small coupling. We denote the dimensionless amplitude of the injected field by $A_e=\sqrt{I_e/I}$, where $I=p/\alpha-1$. Ideally, to entrain an array of $N$ identical lasers requires an injected field amplitude $A_{\mathrm{entr}}=4|\kappa|$, or $E_{\mathrm{entr}}=4|\kappa|\sqrt{I}$. The functional form of the total output intensity may significantly depend on the parameters of the array (such as detunings and the coupling constant). In Fig. 1, we show the normalized total intensity $[I_{\mathrm{tot}}=(1/4I)|(E_1+E_2)|^2]$ of two coupled lasers at the center of the far-field lobe as a function of $A_e$. The injected field frequency approximately corresponds to the average of frequencies of each laser, thus it is tuned to minimize the detunings from the cavity resonances. We continuously vary the strength of the injected field to mimic an experiment where the injected field is gradually increased. Initially, the total intensity grows with the injected field. When the injection strength reaches the critical amplitude, $A_c$, the total intensity drops discontinuously to a significantly lower level [21]. We notice that, just below $A_c$, the total output intensity of the array is about 70% of the maximum intensity (at full entrainment), but requires only about 20% of the entrainment injected field, $E_{\mathrm{entr}}$. We estimate that if we apply a different set of initial conditions, the probability to obtain qualitatively very similar behavior, as demonstrated in Fig. 1, is in the vicinity of 60%. Our estimation is based on simulating a sample of 500 realizations of distinct initial conditions. In the inset of Fig. 1, we present the *averaged* value of the normalized total intensity of two coupled lasers versus the dimensionless amplitude of the external field, $A_e=\sqrt{I_e/I}$. The curve is obtained by numerically solving Eqs. (2) for two coupled lasers and averaging over 500 realizations of the initial conditions.

A characteristic feature of independent solid-state lasers (i.e., without coupling and external field) is that, for any initial data their intensities and gains relax to a stationary state $(I,G)=(p/\alpha-1,\alpha)$, i.e., the amplitudes $|I_j-I|$ and $|G_j-G|$ decay to zero. Numerical experiments [7], using physically realistic parameter values, show similar transient behavior of intensities and gains in the full laser array system (2), where both coupling and excitation terms are present. Once these transients have decayed, it turns out that the dynamics of the phases $\phi_j$ no longer depend on intensities. This motivates, at least at a heuristic level, the use of phase equations in Eqs. (2), with $I_j=I$, as an approximation model to the full system (2). It turns out that the phase equations retain the essential features of the dynamics and can be used to explain the nonmonotonic behavior displayed by the solution of the complete system (2).

We first present a derivation of the phase equations based on averaging theory [22,23]. Our derivation is somewhat technical, including some rescaling of variables whose motivation is not obvious *a priori*. A consequence of this analysis is that it significantly widens the range of validity of the phase model as compared with an earlier derivation based on singular perturbation techniques [17]. Indeed, the simulations depicted in Fig. 1 correspond to a different (significantly expanded) parameter regime, and as we show below, can be completely understood in terms of the reduced phase model.

Substituting $I_j=I(x_j+1)$ $(x_j>-1)$, $G_j=\beta y_j+\alpha$ $(j=1,2)$, $t'=\omega\Omega t$, $\delta_1=\varepsilon\Omega\Delta_1$, $\delta_2=\varepsilon\Omega\Delta_2$, $\kappa=-\varepsilon\Omega$, $A=(1/|\kappa|)\sqrt{I_e/I}$, and $\omega=\alpha/\beta$ with $\beta=\sqrt{(p-\alpha)\omega_0}$, and $\Omega=\beta^2/\alpha$, we transform system (2) into

$$\frac{dx_j}{dt'}=y_j(x_j+1)+\frac{2\varepsilon}{\omega}[-\sqrt{(x_j+1)(x_{j+1}+1)}\cos(\phi_{j+1}-\phi_j)+A\sqrt{x_j+1}\cos\phi_j],$$

$$\frac{dy_j}{dt'}=-x_j-\frac{1}{\omega}y_j\left(\frac{p}{p-\alpha}+x_j\right), \quad (3)$$

$$\frac{d\phi_j}{dt'}=\frac{\varepsilon}{\omega}\left[\Delta_j-\left(\sqrt{\frac{x_{j+1}+1}{x_j+1}}\sin(\phi_{j+1}-\phi_j)-A\frac{1}{\sqrt{x_j+1}}\sin\phi_j\right)\right],$$

where here and henceforth $j=1,2$, and cyclic conditions are imposed ($x_3 \equiv x_1$).

The advantage of this form is that it makes the separation of time scales more transparent. We now assume that $\omega \gg \max(1,\varepsilon)$, where $\omega=\alpha/\sqrt{(p-\alpha)\omega_0}$, and $\varepsilon=-\kappa\alpha/(p-\alpha)\omega_0$. For the set of parameters chosen above (that correspond to experimentally measurable parameters for the Nd:YAG laser [5]), $\omega=200$ and $\varepsilon=40$. Therefore, we satisfy this assumption if $|\kappa| \ll 5\times 10^{-5}$ which, indeed, is satisfied in our simulations since we use $|\kappa|=10^{-5}$ [24]. Then system (3) can be regarded as a perturbation, via damping and coupling terms, of the system with two trivial integrals of motion $\phi_1=\phi_1^0, \phi_2=\phi_2^0$ and two nontrivial integrals $R_1=L(x_1,y_1), R_2=L(x_2,y_2)$ [25], where

$$L(x,y)=\frac{1}{2}y^2+x-\ln(x+1) \tag{4}$$

($x>-1$). Since the level curves $L(x_i,y_i)=R_i$ ($i=1,2$) are ovals surrounding the origin, we can use $R_i$ and a polar angle $\theta_i$ as new coordinates on the $(x_i,y_i)$ plane so that $x_i=x(R_i,\theta_i)$, $y_i=y(R_i,\theta_i)$. In the perturbed system (3), we have $dR_i/dt'=O(1/\omega)$, $d\phi_i/dt'=O(1/\omega)$, and $d\theta_i/dt'=O(1)$. This allows us to write approximate equations for the evolution of amplitudes $R_i$ and phases $\phi_i$ by averaging the true equations over angular variables $\theta_i$. The averaged equations read as follows:

$$\begin{aligned}\frac{dR_j}{dt'}&=-\frac{1}{\omega}K(R_j)+\frac{2\varepsilon}{\omega}L(R_j)[M(R_{j+1})\cos(\phi_{j+1}-\phi_j)\\&\quad -A\cos\phi_j],\\ \frac{d\phi_j}{dt'}&=\frac{\varepsilon}{\omega}\{\Delta_j+N(R_j)[M(R_{j+1})\sin(\phi_j-\phi_{j+1})-A\sin\phi_j]\},\end{aligned} \tag{5}$$

where

$$K(r)=\frac{1}{2\pi}\int_0^{2\pi} y^2(r,\theta)\left(\frac{p}{p-\alpha}+x(r,\theta)\right)d\theta$$

$$[K(r)>0 \quad \text{for} \quad r>0],$$

$$L(r)=-\frac{1}{2\pi}\int_0^{2\pi}\frac{x(r,\theta)}{\sqrt{x(r,\theta)+1}}d\theta,$$

$$M(r)=\frac{1}{2\pi}\int_0^{2\pi}\sqrt{x(r,\theta)+1}\,d\theta,$$

and

$$N(r)=\frac{1}{2\pi}\int_0^{2\pi}\frac{1}{\sqrt{x(r,\theta)+1}}d\theta.$$

In the asymptotic limit, $(R_1,R_2)$ tend to $(0,0)$, provided their initial values lie within certain bounds. Indeed, by computing the leading terms of $K(r)$, $L(r)$, $M(r)$, and $N(r)$ near $r=0$, we get $L(x,y)=\frac{1}{2}y^2+\frac{1}{2}x^2+O(r^{3/2})$ yielding $x=\sqrt{2r}\cos\theta+O(r)$, $y=\sqrt{2r}\sin\theta+O(r)$, and $K(r)=\frac{3}{2}r+O(r^2)$, $L(r)=\frac{1}{4}r+O(r^2)$, $M(r)=1+O(r^2)$, and $N(r)=1+O(r^2)$. Given $p,\xi,c,r_0$ ($r_0>0$), we can always choose $\varepsilon>0$ (not necessarily small) such that $dR_1/dt'<0$, $dR_2/dt'<0$ in the domain $R_1 \leqslant r_0$, $R_2 \leqslant r_0$. This implies asymptotic stability of the origin in the plane $(R_1,R_2)$ for the averaged equations (5). Neglecting $O(r^2)$ terms in the averaged equations (5) for phases and redefining parameters, we obtain the phase model

$$\begin{aligned}\dot\phi_1&=\delta_j+\kappa\sin(\phi_2-\phi_1)-A_e\sin\phi_1,\\ \dot\phi_2&=\delta_2+\kappa\sin(\phi_1-\phi_2)-A_e\sin\phi_2.\end{aligned} \tag{6}$$

Equations (6) provide a significantly reduced description which captures nevertheless the essential dynamics, including the sudden drop in output intensity depicted in Fig. 1, as we now show. We write Eqs. (6) in the following form:

$$\begin{aligned}\frac{d}{dt}(\phi_1+\phi_2)&=\delta_1+\delta_2-A_e(\sin\phi_1+\sin\phi_2),\\ \frac{d}{dt}(\phi_1-\phi_2)&=\delta_1-\delta_2+2\kappa\sin(\phi_2-\phi_1)\\&\quad +A_e(\sin\phi_2-\sin\phi_1).\end{aligned} \tag{7}$$

The frequency of the external field is tuned to minimize the detunings from the cavity resonances, thus we may assume $(\delta_1+\delta_2)\approx 0$. This allows us to reduce the dimensionality of the parameter space and essentially carry out the (simplified) analysis of the dynamics and of the fixed points in the plane $(\delta_1-\delta_2,\kappa)$. Thus, with these assumptions [26], the stationary form of Eqs. (7) reads

$$\begin{aligned}&\sin\phi_1+\sin\phi_2=0,\\ &\delta_1-\delta_2+2\kappa\sin(\phi_2-\phi_1)+A_e(\sin\phi_2-\sin\phi_1)=0.\end{aligned} \tag{8}$$

The first equation in Eqs. (8) implies that either (a) $\phi_2-\phi_1=(2m+1)\pi$, or (b) $\phi_1+\phi_2=2\pi m$, where $m$ is an integer ($m=0,1,2,\ldots$). Solutions of class (a) imply $\sin(\phi_2-\phi_1)=0$, yielding $\sin\phi_1=\delta_1/A_e$, $\sin\phi_2=\delta_2/A_e$, and $\sin(\phi_1-\phi_2)=\sin[\sin^{-1}(\delta_1/A_e)-\sin^{-1}(\delta_2/A_e)]\neq 0$, i.e., inconsistency. Hence, the only possibility is the class (b) of solutions which, in turn, can be divided into two subclasses: $m$ even and $m$ odd. For $m$ even, the second equation in Eqs. (8) becomes

$$f(\phi)\equiv-\delta-2\kappa\sin\phi-2A_e\sin\frac{\phi}{2}=0, \tag{9}$$

where we substituted $\delta=\delta_1-\delta_2$ and $\phi=\phi_2-\phi_1$.

For small values of $A_e$, this equation has two solutions, one stable and one unstable. By increasing the strength of the injected field $A_e$, a saddle-node bifurcation occurs at a critical value, $A_c$.

For $A_e>A_c$, Eq. (9) has no real solution. To determine $A_c$, we solve the system $f(\phi)=0$ and $f'(\phi)=0$,

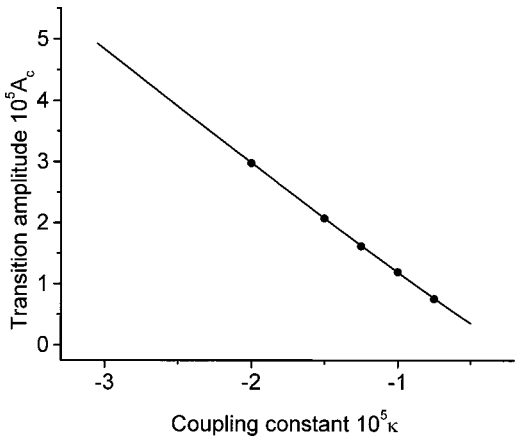


FIG. 2. The critical amplitude, $A_c$, as a function of the coupling strength, $\kappa$. The solid line is the theoretical curve, while the points are the results of numerical calculations [Eq. (2)]. The other parameters are the same as in Fig. 1. All units are dimensionless.

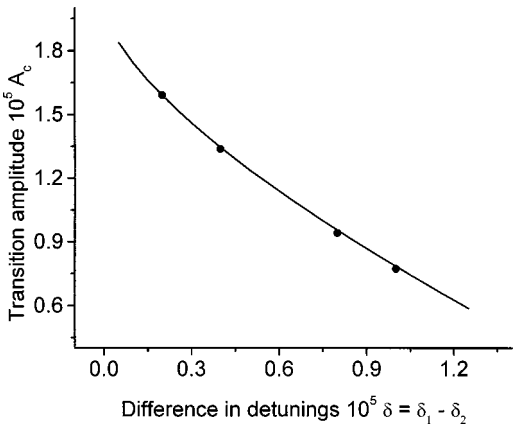


FIG. 3. The critical amplitude, $A_c$, as a function of the differences in detuning, $\delta = \delta_1 - \delta_2$. The solid line is the theoretical curve, while the points are the results of numerical calculations [Eq. (2)]. The other parameters are as in Fig. 1. All units are dimensionless.

namely, $-\delta - 2\kappa \sin\phi_c - 2A_c \sin(\phi_c/2) = 0$ and $-2\kappa \cos\phi_c - A_c \cos(\phi_c/2) = 0$. Making a substitution $\tan(\phi_c/2) = z$ and eliminating $A_c$, we obtain $z^3 + (\delta/4\kappa)z^2 + (\delta/4\kappa) = 0$, with the solution $z = [-(q/2) + \sqrt{D}]^{1/3} + [-(q/2) - \sqrt{D}]^{1/3} - \delta/12\kappa$, where $D = (p/3)^3 + (q/2)^2$, $p = -\delta^2/48\kappa^2$, and $q = (\delta/4\kappa) + (\delta^3/864\kappa^3)$. Substituting the expression for $z$ in the equations above yields an expression for $A_c$:

$$A_c = -2\kappa \frac{1 - z^2}{\sqrt{(1 + z^2}}. \tag{10}$$

Omitting the (very small) higher order terms in $\delta/\kappa$ yields the simple but accurate approximation $z_c = (\delta/-4\kappa)^{1/3} - (\delta/12\kappa)$.

For $m$ odd, the second equation in Eqs. (8) reads

$$g(\phi) \equiv -\delta - 2\kappa \sin\phi + 2A_e \sin\frac{\phi}{2} = 0. \tag{11}$$

A similar analysis shows that this equation has two solutions, one close to $\phi \approx 0$ and the other close to $\phi \approx \pi$. The stability of these solutions is determined by checking the sign of $g'(\phi)$. Since $g'(0) > 0$ and $g'(\pi) < 0$, the solution $\phi \approx 0$ is unstable, while $\phi \approx \pi$ is stable. At small values of the amplitude of the injected field $A_e$, the system has two stable solutions, one close to $\pi/2$ that solves Eq. (9) and one close to $\pi$ that solves Eq. (11). Since the total output intensity is given by $I_{\text{tot}} = 4\cos^2(\phi/2)$ [27], one solution has high intensity while the other one has low intensity.

Each of these stable solutions has a basin of attraction and the selection of the solution depends, of course, on the initial conditions. When $A_e = A_c$, the high-intensity solution disappears at the saddle-node point and for higher values of $A_c$ only the low-intensity solution remains.

In Fig. 2, we show the critical amplitude $A_c$ as a function of the coupling strength $\kappa$ for fixed $z$. The solid line is obtained based on the analytical expression [Eq. (10)], while the points are determined from the solution of the full set of equations [Eqs. (2)]. We notice that the fit between the numerical and analytical expressions is excellent. We also calculated the dependence of the critical amplitude $A_c$ on the diffference in detunings $\delta_1 - \delta_2 \equiv \delta$. The outcome is presented in Fig. 3, where the solid line shows the analytical expression [Eq. (10)] while the points are the result of the numerical simulations. As in Fig. 2, we obtain an almost perfect agreement.

In summary, we have demonstrated that the far-field total intensity at the center of the lobe, $I_{\text{tot}}$, exhibits nonmonotonic behavior as a function of the injected field. Initially the total intensity grows but, at a critical injection amplitude, $A_c$, it undergoes a sharp transition to a lower intensity branch. This behavior can be analytically explained by the reduced ''phase model'' of the array. For the parameter values considered in this paper, one can achieve a significant partial entrainment of the array—up to 70% of the maximum intensity—with injected fields about five times smaller than the saturation entrainment field, $E_{\text{entr}}$. This could result in significant reductions of the power required to entrain laser arrays by injection, thereby removing one of the main obstacles that limit the applicability of this technique.

We thank Dr. L. Zhang for his helpful comments and suggestions on the manuscript. This work was partially supported (Y.B. and V.P.) by the Engineering Research Program of the DOE Office of Basic Energy Sciences under Contract No. DE-AC05-96OR22725 with UT-Battelle, LLC, and by the Office of Naval Research (Y.B.). A.I.K. acknowledges the DOE, Grant No. DE-FG02-93-ER251.

[1] N. W. Carlson, *Monolithic Diode-Laser Arrays* (Springer, New York, 1994).
[2] D. Botez and D. E. Ackley, IEEE Circuits Devices Mag. **2**, 8 (1986).
[3] V. V. Likhanskii and A. P. Napartovich, Usp. Fiz. Nauk **160**, 101 (1990) [Sov. Phys. Usp. **33**, 228 (1990)].
[4] S. Shakir and W. W. Chow, Phys. Rev. A **32**, 983 (1985).
[5] L. Fabiny, P. Colet, R. Roy, and D. Lenstra, Phys. Rev. A **47**, 4287 (1993).
[6] M. Silber, L. Fabiny, and K. Wiesenfeld, J. Opt. Soc. Am. B **10**, 1121 (1993).
[7] Y. Braiman, T. A. B. Kennedy, K. Wiesenfeld, and A. Khibnik, Phys. Rev. A **52**, 1500 (1995).
[8] S. S. Wang and H. G. Winful, Appl. Phys. Lett. **52**, 1774 (1988); H. G. Winful and S. S. Wang, *ibid.* **53**, 1894 (1988).
[9] H. Adachihara, O. Hess, R. Indik, and J. V. Moloney, J. Opt. Soc. Am. B **10**, 496 (1993); P. Ru, P. K. Jakobsen, J. V. Moloney, and R. A. Indik, *ibid.* **10**, 507 (1993).
[10] R. D. Li and T. Erneux, Phys. Rev. A **46**, 4252 (1992); **49**, 1301 (1994).
[11] J. Mercier and M. McCall, Opt. Commun. **138**, 200 (1997); **119**, 576 (1995).
[12] A. Hohl, A. Gavrielides, T. Erneux, and V. Kovanis, Phys. Rev. Lett. **78**, 4745 (1997); A. Gavrielides, V. Kovanis, P. M. Varangis, T. Erneux, and G. Lythe, Quantum Semiclassic. Opt. **9**, 785 (1997).
[13] A. Hohl, A. Gavrielides, T. Erneux, and V. Kovanis, Phys. Rev. A **59**, 3941 (1999); A. Barsella, C. Lepers, D. Dangoisse, P. Glorieux, and T. Erneux, Opt. Commun. **165**, 251 (1999); M. Möller, B. Forsmann, and W. Lange, Chaos, Solitons Fractals **10**, 825 (1999); M. Möller, B. Forsmann, and W. Lange, Quantum Semiclassic. Opt. **10**, 839 (1998); K. S. Thornburg, Jr., M. Möller, R. Roy, T. W. Carr, R.-D. Li, and T. Erneux, Phys. Rev. E **55**, 3865 (1997).
[14] G. D. VanWiggeren and R. Roy, Science **279**, 5354 (1998); S. Sivaprakasam and K. A. Shore, Opt. Lett. **24**, 1200 (1999).
[15] L. Goldberg, H. F. Taylor, J. F. Weller, and D. R. Scifres, Appl. Phys. Lett. **46**, 236 (1985).
[16] M. K. Chun, L. Goldberg, and J. F. Weller, Opt. Lett. **14**, 272 (1989).
[17] A. I. Khibnik, Y. Braiman, T. A. B. Kennedy, and K. Wiesenfeld, Physica D **111**, 295 (1998).
[18] O. Braun, M. Palyi, and B. Hu, Phys. Rev. Lett. **83**, 5206 (1999).
[19] H. Sakaguchi, Prog. Theor. Phys. **79**, l39 (1988).
[20] M. K. S. Yeung and S. H. Strogatz, Phys. Rev. E **58**, 4421 (1998).
[21] The amplitude dropout effect will lead to a significant decrease of the intensity at the far-field central lobe and to amplification of the intensity of double peaks that are symmetric to the center of the pattern. It will not be a ''pure'' antiphase pattern since, because of partial entrainment by the injected field, approximately 25% of the total intensity is concentrated at the center lobe.
[22] V. I. Arnol'd, *Geometric Methods in the Theory of Ordinary Differential Equations* (Springer, New York, 1983).
[23] J. A. Sanders and F. Verhulst, *Averaging Methods in Nonlinear Dynamical Systems* (Springer, New York, 1985).
[24] Note that in Ref. [17], we requested $\varepsilon \ll 1$, which corresponds to $|\kappa| \ll 2.5 \times 10^{-7}$.
[25] H. G. Solari and G. L. Oppo, Opt. Commun. **111**, 173 (1994).
[26] To be consistent with the numerical investigations, which are done for $(\delta_1 + \delta_2) \approx 0$, one should actually consider perturbation analysis, but this is not within the scope of this paper and, based on our numerical results, it would not alter its main conclusions.
[27] The total output intensity (in the units of the intensity of a single uncoupled laser) is given by

$$\begin{aligned} I_{\mathrm{tot}}/I &= (\sin\phi_1 + \sin\phi_2)^2 + (\cos\phi_1 + \cos\phi_2)^2 \\ &= 4\sin^2[(\phi_1+\phi_2)/2]\cos^2[(\phi_1-\phi_2)/2] \\ &\quad + 4\cos^2[(\phi_1+\phi_2)/2]\cos^2[(\phi_1-\phi_2)/2] \\ &= 4\cos^2[(\phi_1-\phi_2)/2] \end{aligned}$$

since, for class (b) solutions, we consider $\phi_1 + \phi_2 = 2\pi m$. The normalized total output intensity $I_{\mathrm{tot}}/(IN^2) = \cos^2[(\phi_1 - \phi_2)/2]$ since $N^2 = 4$. For the case of total entrainment ($\phi_1 = \phi_2$), $I_{\mathrm{tot}}/(IN^2) = 1$, and $I_{\mathrm{tot}}/N^2 = I = p/\alpha - 1 = 1/2$.